Fizika Nizkikh Temperatur, 2004, v. 30, Nos. 7/8, p. 738–755

Charge and spin effects in mesoscopic Josephson junctions

(**Review Article**)

Ilya V. Krive[1,2], Sergei I. Kulinich[1,2], Robert I. Shekhter[1], and Mats Jonson[1]

[1]*Department of Applied Physics, Chalmers University of Technology Göteborg University, SE-412 96 Göteborg, Sweden*

[2]*B. Verkin Institute for Low Temperature Physics and Engineering of the National Academy of Sciences of Ukraine, 47 Lenin Ave., Kharkov 61103, Ukraine*
E-mail: Shekhter@fy.chalmers.se

Received January 30, 2004

We consider the charge and spin effects in low dimensional superconducting weak links. The first part of the review deals with the effects of electron–electron interaction in Superconductor/Luttinger liquid/Superconductor junctions. The experimental realization of this mesoscopic hybrid system can be the individual single wall carbon nanotube that bridges the gap between two bulk superconductors. The dc Josephson current through a Luttinger liquid is evaluated in the limits of perfectly and poorly transmitting junctions. The relationship between the Josephson effect in a long SNS junction and the Casimir effect is discussed. In the second part of the paper we review the recent results concerning the influence of the Zeeman and Rashba interactions on the thermodynamical properties of ballistic S–QW–S junction fabricated in two dimensional electron gas. It is shown that in magnetically controlled junction there are conditions for resonant Cooper pair transition which results in giant supercurrent through a tunnel junction and a giant magnetic response of a multichannel SNS junction. The supercurrent induced by the joint action of the Zeeman and Rashba interactions in 1D quantum wires connected to bulk superconductors is predicted.

PACS: 71.10.Pm, 72.15.Nj, 73.21.Hb, **73.23.–b**, **74.50.+r**

Contents

1. Introduction

Since the discovery of superconductivity in 1911 this amazing macroscopic quantum phenomena has influenced modern solid state physics more then any other fundamental discovery in the 20th century. The mere fact that five Nobel prizes already have been awarded for discoveries directly connected to superconductivity indicates the worldwide recognition of the exceptional role superconductivity plays in physics.

Both at the early stages of the field development and later on, research in basic superconductivity brought surprises. One of the most fundamental discoveries made in superconductivity was the Josephson effect [1]. In 1962 Josephson predicted that when two superconductors are put into contact via an insulating layer (SIS junction) then (i) a dc supercurrent $J = J_c \sin\varphi$ (J_c is the critical current, φ is the superconducting phase difference) flows through the junction in equilibrium (dc Josephson effect) and (ii) an alternating current ($\varphi = \omega_J t$, $\omega_J = 2eV/\hbar$, where V is the bias voltage) appears when a voltage is applied across the junction (ac Josephson effect). A year latter both the dc and the ac Josephson effect were observed in experiments [2,3]. An important contribution to the experimental proof of the Josephson effect has been made by Yanson, Svistunov, and Dmitrenko [4], who were the first to observe rf-radiation from the voltage biased contact and who measured the temperature dependence of the critical Josephson current $J_c(T)$.

As a matter of fact the discovery of the Josephson effect gave birth to a new and unexpected direction in superconductivity, namely, the superconductivity of weak links (weak superconductivity, see, e.g., Ref. 5). It soon became clear that any normal metal layer between superconductors (say, an SNS junction) will support a supercurrent as long as the phase coherence in the normal part of the device is preserved. Using the modern physical language one can say that the physics of superconducting weak links turned out to be part of mesoscopic physics.

During the last decade the field of mesoscopic physics has been the subject of an extraordinary growth and development. This was mainly caused by the recent advances in fabrication technology and by the discovery of principally new types of mesoscopic systems such as carbon nanotubes (see, e.g., Ref. 6).

For our purposes metallic single wall carbon nanotubes (SWNT) are of primary interest since they are strictly one-dimensional conductors. It was experimentally demonstrated [7–9] (see also Ref. 10) that electron transport along metallic individual SWNT at the low bias voltage regime is ballistic. At first glance this observation looks surprising. For a long time it was known (see Ref. 11) that 1D metals are unstable with respect to the Peierls phase transition, which opens up a gap in the electron spectrum at the Fermi level. In carbon nanotubes the electron–phonon coupling for conducting electrons is very weak while the Coulomb correlations are strong. The theory of metallic carbon nanotubes [12,13] shows that at temperatures outside the mK-range the individual SWNT has to demonstrate the properties of a two channel, spin-1/2 Luttinger liquid (LL). This theoretical prediction was soon confirmed by transport measurements on metal-SWNT and SWNT–SWNT junctions [14,15] (see also Ref. 16, where the photoemission measurements on a SWNT were interpreted as a direct observation of LL state in carbon nanotubes). Both theory and experiments revealed strong electron–electron correlations in SWNTs.

Undoped individual SWNT is not intrinsically a superconducting material. Intrinsic superconductivity was observed only in ropes of SWNT (see Refs. 17 and 18). Here we consider the proximity-induced superconductivity in a LL wire coupled to superconductors (SLLS). The experimental realization of SLLS junction could be an individual SWNT, which bridges the gap between two bulk superconductors [19,20].

The dc Josephson current through a LL junction was evaluated for the first time in Ref. 21. In this paper a tunnel junction was considered in the geometry (see subsection 2.2.), which is very suitable for theoretical calculations but probably difficult to realize in an experiment. It was shown that the Coulomb correlations in a LL wire strongly suppress the critical Josephson current. The opposite limit — a perfectly transmitting SLLS junction was studied in Ref. 22, where it was demonstrated by a direct calculation of the dc Josephson current that the interaction does not renormalize the supercurrent in a fully transparent ($D = 1$, D is the junction transparency) junction. In subsection 2.2. we re-derive and explain these results using the boundary Hamiltonian method [23].

The physics of quantum wires is not reduced to the investigations of SWNTs. Quantum wires can be fabricated in a two-dimensional electron gas (2DEG) by using various experimental methods. Some of them (e.g., the split-gate technique) originate from the end of 80's when the first transport experiments with a quantum point contact (QPC) revealed unexpected properties of quantized electron ballistic transport (see, e.g., Ref. 24). In subsection 2.1. we briefly review the results concerning the quantization of the critical supercurrent in a QPC.

In quantum wires formed in a 2DEG the electron–electron interaction is less pronounced [25] than in SWNTs (presumably due to the screening effects of nearby bulk metallic electrodes). The electron transport in these systems can in many cases be

successfully described by Fermi liquid theory. For noninteracting quasiparticles the supercurrent in a SNS ballistic junction is carried by Andreev levels. For a long ($L >> \xi_0 = \hbar v_F/\Delta$, L is the junction length, Δ is the superconducting energy gap) perfectly transmitting junction the Andreev–Kulik spectrum [26] for quasiparticle energies $E << \Delta$ is a set of equidistant levels. In subsection 2.3. we show that this spectrum corresponds to twisted periodic boundary conditions for chiral (right- and left-moving) electron fields and calculate the thermodynamic potential of an SNS junction using field theoretical methods. In this approach there is a close connection between the Josephson effect and the Casimir effect.

In Section 3 of our review we consider the spin effects in ballistic Josephson junctions. As is well-known, the electron spin does not influence the physics of standard SIS or SNS junctions. Spin effects become significant for SFS junctions (here «F» denotes a magnetic material) or when spin-dependent scattering on magnetic impurities is considered. As a rule, magnetic impurities tend to suppress the critical current in Josephson junction by inducing spin-flip processes [27,28]. Another system where spin effects play an important role is a quantum dot (QD). Intriguing new physics appears in normal and superconducting charge transport through a QD at very low temperatures when the Kondo physics starts to play a crucial role in the electron dynamics. Last year a vast literature was devoted to these problems.

Here we discuss the spin effects in a ballistic SNS junction in the presence of: (i) the Zeeman splitting due to a local magnetic field acting only on the normal part of the junction, and (ii) strong spin-orbit interaction, which is known to exist in quantum heterostructures due to the asymmetry of the electrical confining potential [29]. It is shown in subsection 3.1. that in magnetically controlled single barrier junction there are conditions when superconductivity in the leads strongly enhances electron transport, so that a giant critical Josephson current appears $J_c \sim \sqrt{D}$. The effect is due to resonant electron transport through de Gennes–Saint–James energy levels split by tunneling.

The joint action of Zeeman splitting and superconductivity (see subsection 3.2.) results in yet another unexpected effect — a giant magnetic response, $M \sim N_\perp \mu_B$, (M is the magnetization, $N_\perp$ is the number of transverse channels of the wire, μ_B is the Bohr magneton) of a multichannel quantum wire coupled to superconductors [30]. This effect can be understood in terms of the Andreev level structure which gives rise to an additional (superconductivity-induced) contribution to the magnetization of the junction. The magnetization peaks at special values of the superconducting phase difference when the Andreev energy levels at $E_\pm = \pm\Delta_Z$, (Δ_Z is the Zeeman energy splitting) become $2N_\perp$-fold degenerate.

The last two subsections of Sec. 3 deal with the influence of the Rashba effect on the transport properties of quasi-1D quantum wires. Strong spin–orbit (SO) interaction experienced by 2D electrons in heterostructures in the presence of additional lateral confinement results in a dispersion asymmetry of the electron spectrum in a quantum wire and in a strong correlation between the direction of electron motion along the wire (right/left) and the electron spin projection [31,32].

The chiral properties of electrons in a quantum wire cause nontrivial effects when the wire is coupled to bulk superconductors. In particular, in subsection 3.4. we show that the Zeeman splitting in a S–QW–S junction induces an anomalous supercurrent, that is a Josephson current that persists even at zero phase difference between the superconducting banks.

In Conclusion we once more emphasize the new features of the Josephson current in ballistic mesoscopic structures and briefly discuss the novel effects, which could appear in an ac Josephson current through an ultra-small superconducting quantum dot.

2. Josephson current through a superconductor—quantum wire—superconductor junction

In this chapter we consider the Josephson current in a quantum wire coupled to bulk superconductors. One could expect that the conducting properties of this system strongly depend on the quality of the electrical contacts between the QW and the superconductors. The normal conductance of a QW coupled to electron reservoirs in Fermi liquid theory is determined by the transmission properties of the wire (see, e.g., Ref. 33). For the ballistic case the transmission coefficient of the system in the general situation of nonresonant electron transport depends only on the transparencies of the potential barriers which characterize the electrical contacts and does not depend on the length L of the wire. As already was mentioned in the Introduction, the Coulomb interaction in a long 1D (or few transverse channel) QW is strong enough to convert the conduction electrons in the wire into a Luttinger liquid. Then the barriers at the interfaces between QW and electron reservoirs are strongly renormalized by electron–electron interaction and the conductance of the N–QW–N junction at low temperature strongly depends on the wire length [34]. For a long junction and repulsive electron–electron interaction the current through the system is strongly suppressed. The only exception is the case of perfect (adiabatic) contacts when the backscattering of electrons at the interfaces is negligibly (exponentially)

small. In the absence of electron backscattering the conductance G is not renormalized by interaction [35] and coincides with the conductance quantum $G = 2e^2/h$ (per channel). From the theory of Luttinger liquids it is also known [36] that for a strong repulsive interaction the resonant transition of electrons through a double-barrier structure is absent even for symmetric barriers.

The well-known results for the transport properties of 1D Luttinger liquid listed above (see, e.g., Rev. 37) allows us to consider two cases when studing ballistic S–QW–S junctions: (i) a transparent junction ($D = 1$), and (ii) a tunnel junction ($D << 1$). These two limiting cases are sufficient to describe the most significant physical effects in S–QW–S junctions.

2.1. Quantization of the Josephson current in a short ballistic junction

At first we consider a short $L << \xi_0$; ballistic S–QW–S junction. One of the realizations of this mesoscopic device is a quantum point contact (QPC) in a 2DEG (see Fig. 1,*a*). For a QPC the screening of the Coulomb interaction is qualitatively the same as in a pure 2D geometry and one can evaluate the Josephson current through the constriction in a noninteracting electron model. Then due to Andreev backscattering of quasiparticles at the SN interfaces, a set of Andreev levels is formed in the normal part of the junction [26]. In a single mode short junction the spectrum of bound states takes the form [38] ($L/\xi_0 \to 0$)

$$E_{\pm} = \pm\Delta\sqrt{1 - D\sin^2(\varphi/2)} \qquad (1)$$

where φ is the superconducting phase difference. This spectrum does not depend on the Fermi velocity and therefore the Andreev levels, Eq.(1), in a junction with $N_{\perp}$ transverse channels are $2N_{\perp}$ degenerate (the factor 2 is due to spin degeneracy).

It is well known (see, e.g., Refs. 39 and 40) that the continuum spectrum in the limit $L/\xi_0 \to 0$ does not contribute to the Josephson current,

$$J = \frac{e}{\hbar}\frac{\partial\Omega}{\partial\varphi}, \qquad (2)$$

where Ω is the thermodynamic potential. It is evident from Eqs. (1) and (2) that the Josephson current through a QPC ($D = 1$) is quantized [39]. At low temperatures ($T << \Delta$) we have [39]

$$J = N_{\perp}\frac{e\Delta}{\hbar}\sin\frac{\varphi}{2}. \qquad (3)$$

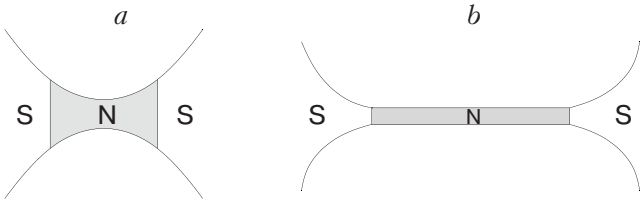

Fig. 1. A schematic display of a superconducting point contact (*a*). Quantum wire adiabatically connected to bulk superconductors (*b*).

This effect⋆ is the analog of the famous conductance quantization in QPCs (see Ref. 41).

Now let us imagine that the geometry of the constriction allows one to treat the QPC as a 1D quantum wire of finite length L smoothly connected to bulk superconductors (Fig. 1,*b*). The 1D wire is still much shorter that the coherence length ξ_0. How does the weakly screened Coulomb interaction in a 1D QW influence the Josephson current in a fully transmitting ($D = 1$) junction? Notice that the charge is freely transported through the junction since the real electrons are not backscattered by the adiabatic constriction [42]. So, it is reasonable to assume that the Coulomb interaction in this case does not influence the Josephson current at all. We will prove this assumption for the case of a long junction in the next section. If the QW is separated from the leads by potential barriers (quite a natural situation in a real experiment) the charging effects have to be taken into account. As a rule the Coulomb correlations, which tend to keep the number of electrons in the normal region (quantum dot in our case) constant, suppress the critical supercurrent due to the Coulomb blockade effect (see, e.g., Ref. 43, where a consistent theory of the Coulomb blockade of Josephson tunneling was developed). They can also change the φ-dependence of the Josephson current. One possible scenario for how charging effects influence the Josephson current in a short SNS junction is considered in Ref. 44.

2.2. Luttinger liquid wire coupled to superconductors

A consistent theory of electron–electron interactions effects in weak superconductivity has been developed for a long 1D or quasi-1D SNS junction, when the normal region can be modelled by a Luttinger liquid (LL). The standard approach to this problem (see, e.g., Ref. 23) is to use for the description of electron transport through the normal region the LL Hamiltonian

⋆ It was recently observed in: T. Bauch et al., *Supercurrent and Conductance Quantization in Superconducting Quantum Point Contact, cond-mat/0405205*, May 11, 2004.

with boundary conditions which take into account the Andreev [45] and normal backscattering of quasiparticles at the NS interfaces.

The LL Hamiltonian H_{LL} expressed in terms of charge density operators $\tilde{\rho}_{R/L,\uparrow/\downarrow}$ of right/left moving electrons with up/down spin projection takes the form (see, e.g., Ref. 46)

$$H_{LL} = \pi\hbar \int dx \,[u(\tilde{\rho}^2_{R\uparrow} + \tilde{\rho}^2_{L\uparrow} + \tilde{\rho}^2_{R\downarrow} + \tilde{\rho}^2_{L\downarrow}) +$$

$$+ \frac{V_0}{\pi\hbar}(\tilde{\rho}_{R\uparrow}\tilde{\rho}_{R\downarrow} + \tilde{\rho}_{L\uparrow}\tilde{\rho}_{L\downarrow} + \tilde{\rho}_{R\uparrow}\tilde{\rho}_{L\uparrow} + \tilde{\rho}_{R\downarrow}\tilde{\rho}_{L\downarrow} + \tilde{\rho}_{R\uparrow}\tilde{\rho}_{L\downarrow} + \tilde{\rho}_{R\downarrow}\tilde{\rho}_{L\uparrow})], \quad (4)$$

where V_0 is the strength of electron–electron interaction ($V_0 \sim e^2$) and the velocity $u = v_F + V_0/2\pi\hbar$. The charge density operators of the chiral (R/L) fields obey anomalous Kac–Moody commutation relations (see, e.g., Ref. 46)

$$[\tilde{\rho}_{R(L)j}(x), \tilde{\rho}_{R(L)k}(x')] =$$

$$= \pm \frac{\delta_{jk}}{2\pi i}\frac{\partial}{\partial x}\delta(x - x'), \quad j,k = \uparrow,\downarrow.$$

The Hamiltonian (4) is quadratic and can easily be diagonalized by a Bogoliubov transformation

$$H^{(d)}_{LL} = \pi\hbar \int dx[v_\rho(\rho^2_{R\rho} + \rho^2_{L\rho}) + v_\sigma(\rho^2_{R\sigma} + \rho^2_{L\sigma})], \quad (5)$$

where $v_{\rho(\sigma)}$ are the velocities of noninteracting bosonic modes (plasmons), $v_{\rho(\sigma)} = v_F/g_{\rho(\sigma)}$, and

$$g_\rho = \left(1 + \frac{2V_0}{\pi\hbar v_F}\right)^{-1/2}, \quad g_\sigma = 1. \quad (6)$$

Here g_ρ and g_σ are the correlation parameters of a spin-1/2 LL in the charge (ρ) and spin (σ) sectors. Notice that $g_\rho << 1$ for a strongly interacting ($V_0 >> \hbar v_F$) electron system.

The Andreev and normal backscattering of quasiparticles at the NS boundaries ($x = 0$ and $x = L$) can be represented by the effective boundary Hamiltonian $H_B = H^{(A)}_B + H^{(N)}_B$

$$H^{(A)}_B = \Delta^{(l)}_B[\Psi_{R\uparrow}(0)\Psi_{L\downarrow}(0) + \Psi_{R\downarrow}(0)\Psi_{L\uparrow}(0)] +$$

$$+ \Delta^{(r)}_B[\Psi_{R\uparrow}(L)\Psi_{L\downarrow}(L) + \Psi_{R\downarrow}(L)\Psi_{L\uparrow}(L)] + \text{h.c.}, \quad (7)$$

$$H^{(N)}_B = V^{(l)}_B \sum_{j,\sigma} \Psi^\dagger_{j\sigma}(0)\Psi_{j\sigma}(0) +$$

$$+ V^{(r)}_B \sum_{j,\sigma} \Psi^\dagger_{j\sigma}(L)\Psi_{j\sigma}(L), \quad (8)$$

where $j = (L,R)$, $\sigma = (\uparrow,\downarrow)$. Here $\Delta^{(l,r)}_B$ is the effective boundary pairing potential at the left (right) NS interface and $V^{(l,r)}_B$ is the effective boundary scattering potential. The values of these potentials are related to the phase of the superconducting order parameters in the banks and to the normal scattering properties at the left and right interfaces. They can be considered either as input parameters (see, e.g., Ref. 47) or they can be calculated by using some particular model of the interfaces [23]. In what follows we will consider two limiting cases: (i) poorly transmitting interfaces $V^{(l,r)}_B \to \infty$ (tunnel junction) and (ii) perfectly transmitting interfaces $V^{(l,r)}_B \to 0$.

At first we relate the effective boundary pairing potentials $\Delta^{(l,r)}_B$ to the amplitudes $r^{(l,r)}_A$ of the Andreev backscattering process [48,49]. Let us consider for example the Andreev backscattering of an electron at the left interface. This process can be described as the annihilation of two electrons with opposite momenta and spin projections at $x = 0$. The corresponding Hamiltonian is $h_A \sim r^{*(l)}_A a_{p,\uparrow} a_{-p,\downarrow}$, or equivalently in the coordinate representation $h_A \sim r^{*(l)}_A \Psi_{R\uparrow}(0)\Psi_{L\downarrow}(0)$. Here r_A is the amplitude of Andreev backscattering at the left interface,

$$r^{(l)}_A = \frac{|t^{(l)}|^2 \exp[i(\varphi_l + \pi/2)]}{\sqrt{|t^{(l)}|^4 + 4|r^{(l)}|^2}}, \quad (9)$$

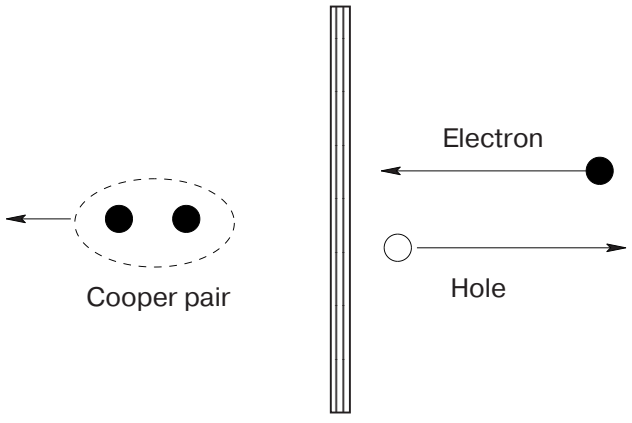

Fig. 2. A schematic picture of Andreev reflection.

$t^{(l)}$ is the transmission amplitude ($|t^{(l)}|^2+|r^{(l)}|^2=1$) and φ_l is the phase of superconducting order parameter at the left bank. An analogous expression holds for the right interface. Notice that for a tunnel junction $|t^{(l,r)}|<<1$ the amplitude of Andreev backscattering is small — it is proportional to the transparency $D_{l,r}\equiv|t^{(l,r)}|^2<<1$ of the barrier at the right (left) interface. So in our model the effective boundary pairing potential is

$$\Delta_B^{(l)}=C\,\hbar v_F r_A^{*(l)},\quad \Delta_B^{(r)}=-C\,\hbar v_F r_A^{*(r)}, \qquad (10)$$

where C is a numerical factor which will be specified later.

2.2.1. Tunnel junction. For poorly transmitting interfaces $D_{r,l}<<1$ the amplitude of Andreev backscattering is small and we can use perturbation theory when evaluating the phase dependent part of the ground state energy. In second order perturbation theory the ground state energy takes the form

$$\delta E^{(2)}(\varphi)=\sum_j \frac{\left|< j\left|H_B^{(A)}\right|0>\right|^2}{E_0-E_j}=$$

$$=\frac{1}{\hbar}\int_0^\infty d\tau <0\left|H_B^{(A)\dagger}(\tau)H_B^{(A)}(0)\right|0>. \qquad (11)$$

Here $H_B^{(A)}(\tau)$ is the boundary Hamiltonian (7) in the imaginary time Heisenberg representation. After substituting Eq. (7) into Eq. (11) we get the following formula for $\delta E^{(2)}$ expressed in terms of electron correlation functions

$$\delta E^{(2)}(\varphi)=-4C\hbar v_F^2\,\mathrm{Re}(r_A^{*(l)}r_A^{(r)}\int_0^\infty d\tau\,[<\Psi_{R\uparrow}(\tau,0)\Psi_{L\downarrow}(\tau,0)\Psi_{L\downarrow}^\dagger(0,L)\Psi_{R\uparrow}^\dagger(0,L)>+<\uparrow\Leftrightarrow\downarrow>]. \qquad (12)$$

We will calculate the electron correlation function by making use of the bosonization technique. The standard bosonisation formula reads

$$\Psi_{\eta,\sigma}(x,t)=\frac{1}{\sqrt{2\pi a}}\exp[i\eta\sqrt{4\pi}\Phi_{\eta,\sigma}(x,t)], \qquad (13)$$

where a is the cutoff parameter ($a\sim\lambda_F$), $\eta=(R,L)\equiv(1,-1)$, $\sigma=(\uparrow,\downarrow)\equiv(1,-1)$. The chiral bosonic fields in Eq. (13) are represented as follows (see, e.g., Ref. 51)

$$\Phi_{\eta,\sigma}(x,t)=\frac{1}{2}\hat\varphi_{\eta,\sigma}+\hat\Pi_\sigma\frac{x-\eta vt}{L}+\varphi_{\eta,\sigma}(x,t). \qquad (14)$$

Here the zero mode operators $\hat\varphi_{\eta,\sigma},\hat\Pi_\sigma$ obey the standard commutation relations for «coordinate» and «momentum» $[\hat\varphi_{\eta,\sigma},\hat\Pi_{\sigma'}]=-i\eta\delta_{\sigma,\sigma'}$. They are introduced for a finite length LL to restore correct canonical commutation relations for bosonic fields [50,51]. Notice that the topological modes associated with these operators fully determine the Josephson current in a transparent ($D=1$) SLLS junction [22]. The nontopological components $\varphi_{\eta,\sigma}(x,t)$ of the chiral scalar fields are represented by the series

$$\varphi_{\eta,\sigma}(x,t)=\sum_q\frac{1}{\sqrt{2qL}}\{\exp[iq(\eta x-vt)]\hat b_q+\mathrm{h.c.}\}, \qquad (15)$$

where $\hat b_q(\hat b_q^\dagger)$ are the standard bosonic annihilation (creation) operator; L is the length of the junction, v is the velocity.

It is convenient here to introduce [46] the charge (ρ) and spin (σ) bosonic fields $\varphi_\sigma,\theta_\rho$, which are related to above defined chiral fields $\varphi_{\eta,\sigma}$ by simple linear equation

$$\begin{pmatrix}\varphi_\sigma\\ \theta_\rho\end{pmatrix}=\frac{1}{\sqrt{2}}(\varphi_{R\uparrow}\pm\varphi_{L\uparrow}\mp\varphi_{R\downarrow}-\varphi_{L\downarrow}) \qquad (16)$$

(the upper sign corresponds to φ_σ and the lower sign denotes θ_ρ). After straightforward transformations Eq. (12) takes the form

$$\delta E^{(2)}(\varphi)=4C\,\hbar v_F^2 D\cos\varphi\int_0^\infty d\tau\,[\Pi_+(\tau)+\Pi_-(\tau)], \qquad (17)$$

where $D=D_lD_r<<1$ is the junction transparency and

$$\Pi_\pm(\tau)=(2\pi a^2)^{-2}\exp\{2\pi[<<\varphi_\sigma(\tau,-L)\varphi_\sigma>>+$$
$$+<<\theta_\rho(\tau,-L)\theta_\rho>>\pm<<\theta_\rho(\tau,-L)\varphi_\sigma>>\pm$$
$$\pm<<\varphi_\sigma(\tau,-L)\theta_\rho>>]\}Q_\pm(\tau). \qquad (18)$$

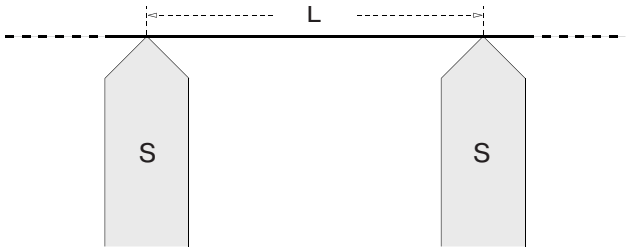

Fig. 3. A schematic picture of a SLLS junction formed by an effectively infinite Luttinger liquid coupled to bulk superconductors by side electrodes.

Here $\varphi_\sigma \equiv \varphi_\sigma(0,0)$, $\theta_\rho \equiv \theta_\rho(0,0)$ and the double brackets << … >> denote the subtraction of the corresponding vacuum average at the points $(\tau, x) = (0,0)$. Note that the superconducting properties of a LL are determined by the correlators of θ_ρ and φ_σ bosonic fields unlike the normal conducting properties where the fields θ_σ and φ_ρ play a dominant role.

The factors $Q_\pm(\tau)$ originate from the contribution of zero modes,

$$Q_\pm(\tau) = \exp\left\{\frac{\pi}{2} < [\hat{\Pi}_\uparrow - \hat{\Pi}_\downarrow \pm \frac{iv_F\tau}{L}(\hat{\Pi}_\uparrow + \hat{\Pi}_\downarrow)]^2 > \right\} \exp(\pi v_F \tau / L). \quad (19)$$

With the help of a Bogoliubov transformation the chiral bosonic fields in Eq. (16) can be expressed in terms of noninteracting plasmonic modes with known propagators (see, e.g., Ref. 46). Two different geometries of SLLS junction have been considered in the literature, viz, an effectively infinite LL connected by the side electrodes to bulk superconductors [21] (see Fig. 3) and a finite LL wire coupled via tunnel barriers to superconductors [47,52]. Notice, that both model geometries can be related to realistic contacts of a single wall carbon nanotube with metals (see, e.g., Ref. 53 and references therein). The geometry of Fig. 3 could model the junction when electron beam lithography is first used to define the leads and then ropes of SWSN are deposited on top of the leads. A tunnel junction of the type schematically shown in Fig. 4 is produced when the contacts are applied over the nanotube rope.

The topological excitations for an effectively infinite LL ($L \to \infty$) play no role and the corresponding contributions can be omitted in Eqs. (15) and (18), $Q_\pm(\tau) \equiv 1$. The propagators of noninteracting chiral bosonic fields are (see, e.g., [46])

$$<< \varphi_{R/L,j}(t,x)\, \varphi_{R/L,k} >> = -\frac{\delta_{jk}}{4\pi} \ln \frac{a \mp x + s_k t}{a}, \quad (20)$$

where $j,k = 1,2$ and the plasmonic velocities $s_1 = v_\rho$, $s_2 = v_\sigma = v_F$ (see Eq.(6)). Finally the expression for the Josephson current through a «side-contacted» LL (Fig. 3) takes the form [21]

$$J_{LL}^{(i)} = J_c^{(0)} R_i(g_\rho) \sin\varphi, \quad (21)$$

where $J_c^{(0)} = (Dev_F/4L)(C/\pi)$ is the critical Josephson current for noninteracting electrons, $R_i(g_\rho)$ is the interaction induced renormalization factor ($R_i(g_\rho = 1) = 1$)

$$R_i(g_\rho) = \frac{g_\rho}{\sqrt{\pi}} \frac{\Gamma(1/2g_\rho)}{\Gamma(1/2 + 1/2g_\rho)} F\left(\frac{1}{2}, \frac{1}{2}; \frac{1}{2g_\rho} + \frac{1}{2}; 1 - g_\rho^2\right) \left(\frac{a}{L}\right)^{g_\rho^{-1} - 1}. \quad (22)$$

Here g_ρ is the correlation parameter of a spin-1/2 LL in the charge sector Eq. (6), $\Gamma(x)$ is the gamma function and $F(\alpha,\beta;\gamma;z)$ is the hypergeometric function (see, e.g., Ref. 54). For the first time the expression for $R_i(g_\rho)$ in the integral form was derived in Ref. 21. In the limit of strong interaction $V_0/\hbar v_F >> 1$ the renormalization factor is small

$$R_i(g_\rho << 1) \simeq \frac{\pi}{2}\left(\frac{\hbar v_F}{V_0}\right)^{3/2} \left(\frac{a}{L}\right)^{\sqrt{2V_0/\pi\hbar v_F}} << 1, \quad (23)$$

and the Josephson current through the SLLS junction is strongly suppressed. This is nothing but a manifestation of the Kane–Fisher effect [34] in the Josephson current.

To evaluate the correlation function, Eq. (18), for a LL wire of finite length coupled to bulk superconductors via tunnel barriers, (Fig. 4), we at first have to formulate boundary conditions for the electron wave function

$$\Psi_\sigma(x) = \exp(ik_F x)\, \Psi_{R,\sigma}(x) + \exp(-ik_F x)\, \Psi_{L,\sigma}(x), \quad \sigma = \uparrow \downarrow \quad (24)$$

at the interfaces $x = 0, L$. To zeroth order of perturbation theory in the barrier transparencies the electrons are confined to the normal region. So the particle current $J_\sigma \sim \mathrm{Re}(i\Psi_\sigma^* \partial_x \Psi_\sigma)$ through the interfaces is

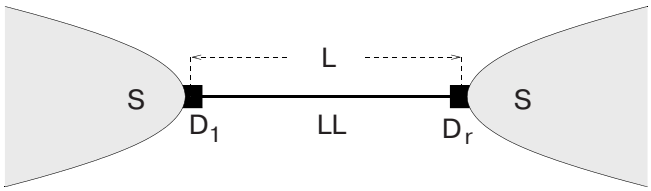

Fig. 4. A Luttinger liquid wire of length L coupled to bulk superconductors via tunnel barriers with transparencies $D_{l(r)}$.

zero. For a single mode LL this requirement is equivalent to the following boundary condition for the chiral fermionic fields [50,52]

$$\Psi^*_{R,\sigma}(x)\Psi_{R,\sigma}(x)|_{x=0,L} = \Psi^*_{L,\sigma}(x)\Psi_{L,\sigma}(x)|_{x=0,L}\cdot \quad (25)$$

These boundary conditions (LL with open ends) result in zero eigenvalues of the «momentum»-like zero mode operator $\hat{\Pi}_\sigma$ and in the quantization of nontopological modes on a ring with circumference $2L$ (see Ref. 50). In this case the plasmon propagators take the form

$$<< \varphi_{L,j}(t,x)\varphi_{RL,k} >> =$$

$$= -\frac{\delta_{jk}}{4\pi}\ln\frac{1-\exp[i\pi(\pm x - s_k t + ia)]}{\pi a/L}. \quad (26)$$

Using Eqs. (2), (17)–(19), and (26) one readily gets the expression for the Josephson current analogous to Eq. (21) $J^{(f)}_{LL} = J^{(0)}_c R_f(g_\rho)\sin\varphi$, where now the critical Josephson current of noninteracting electron is $J^{(0)}_c = (Dev_F/4L)(C/\pi)$ and the renormalization factor ($R_f(g_\rho = 1) = 1$) reads

$$R_f(g_\rho) = \frac{2g_\rho^2}{2-g_\rho^2} F\left(\frac{2}{g_\rho}; \frac{2}{g_\rho} - g_\rho; \frac{2}{g_\rho} - g_\rho + 1, -1\right)\left(\frac{\pi a}{L}\right)^{2(g_\rho^{-1}-1)}. \quad (27)$$

Comparing $J^{(0)}_c$ with the well known formula for the critical Josephson current in a low transparency SINIS junction (see, e.g., Ref. 40) we find the numerical constant $C = \pi$.

In the limit $g_\rho << 1$ of strong interaction Eq. (27) is reduced to the simple formula

$$R_f(g_\rho << 1) \simeq \frac{\pi}{2}\frac{\hbar v_F}{V_0}\left(\frac{\pi a}{L}\right)^{2\sqrt{2V_0/\pi\hbar v_F}} << 1. \quad (28)$$

The dependence of the renormalization factor given by Eqs. (22), (27) on the strength of the electron–electron interaction $V_0/\hbar v_F$ is shown in Fig. 5. The behavior of the Josephson current as a function of the interaction strength is similar for the two considered geometries. However we see that the interaction influences the supercurrent more strongly for the case of «end-coupled» LL wire.

2.2.2. Transparent junction. The case of perfectly transmitting interfaces in terms of the boundary Hamiltonians (7), (8) which formally correspond to the limit $V_B \to 0$ and not small Δ_B. It cannot be treated perturbatively. Physically it means that charge is freely transported through the junction and only pure Andreev reflection takes place at the NS boundaries. It is well known that at energies much smaller than the superconducting gap ($E << \Delta$) the scattering amplitude of quasiparticles becomes energy independent (see Eq. (9)). This enable one to represent the Andreev scattering process as a boundary condition for a real space fermion operator. It was shown in Ref. 22 that the corresponding boundary condition for chiral fermion fields takes the form of a twisted periodic boundary condition over the interval $2L$,

$$\Psi_{L/R,\pm\sigma}(x \pm 2L, t) = \exp(\pm i\vartheta)\Psi_{L/R,\pm\sigma}(x,t) \quad (29)$$

(the upper sign corresponds to the left-moving fermions, lower sign — to right moving particles), where $\vartheta = \pi + \varphi$, φ is the superconducting phase difference and the phase π is acquired due to the Andreev reflection on two interfaces (see, e.g., Eq. (9)). So the problem can be mapped [22] to the one for the persistent current of chiral fermions on a ring of circumference $2L$. It is well known [51,55] (see also the Rev. 56) that the persistent current in a perfect ring (without impurities) in the continuum model does not depend on the electron–electron interaction due to the translational invariance of the problem. This «no-renormalization» theorem allows us to conclude that the Josephson current in a perfectly transmitting SLLS junction coincides with the supercurrent in a one-dimensional long SNS ballistic junction [26,57]

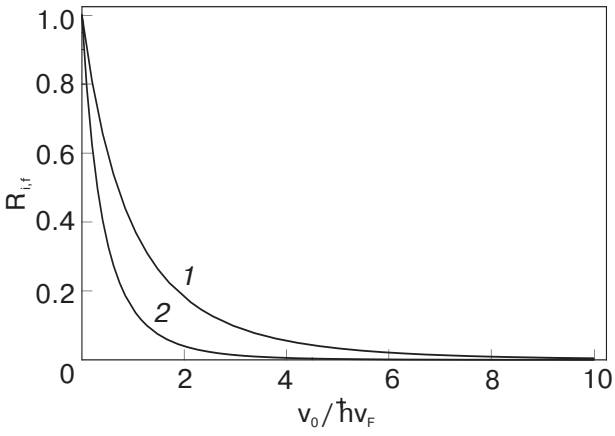

Fig. 5. Dependence of the renormalization factor $R_{i(f)}$ on the dimensionless electron–electron interaction strength $V_0/\hbar v_F$. Curve *1* corresponds to the case of «side-coupled» LL wire (*i*), curve *2* to an «end-coupled» LL wire (*f*).

$$J_{LL} = J_{\text{nonint}} = \frac{4eT}{\hbar}\sum_{k=1}^{\infty}(-1)^{k+1}\frac{\sin k\varphi}{\sinh(2\pi kT/\Delta_L)}, \quad (30)$$

where T is the temperature and $\Delta_L = \hbar v_F/L$. The formal proof of this statement [22] consist in evaluating the partition function of the LL with the twisted boundary conditions, Eq. (29), supplemented by a connection between the $\Psi_{R,\sigma}$ and $\Psi_{L,\sigma}$ fields that follows from the chiral symmetry. The superconducting phase difference φ couples only to zero modes of the charge current field θ_ρ. In a Galilelian invariant system zero modes are not renormalized by the interaction and the partition function for a SLLS junction exactly coincides with the one for a long SNS junction.

We notice here that Eq. (30) holds not only for perfectly transmitting interfaces. It also describes asymptotically at $T << \Delta$ the Josephson current through a tunnel junction when the interaction in the wire is assumed to be attractive. We have seen already in the previous subsection that the electron–electron interaction renormalizies the bare transparency of the junction due to the Kane–Fisher effect. The renormalization is known to suppress the electron current for a repulsive interaction and to enhance it for an attractive forces [34]. So one could expect that for an attractive interaction the electron interface scattering will be renormalized at low temperatures to perfect Andreev scattering [23].

2.3. Josephson current and the Casimir effect

More then fifty years ago Casimir predicted [58] the existence of small quantum forces between grounded metallic plates in vacuum. This force (a kind of van der Waals force between neutral objects) arises due to a change of the vacuum energy (zero-point fluctuations) induced by the boundary conditions imposed by the metallic plates on the fluctuating electromagnetic fields (see Refs. 59 and 60). This force has been measured (see, e.g., one of the recent experiments [61] and the references therein) and in quantum field theory the Casimir effect is considered as the most spectacular manifestation of zero-point energy. In a general situation the shift of the vacuum energy of fluctuating fields in a constrained volume is usually called the Casimir energy E_C. For a field with zero rest mass dimensional considerations result in a simple behavior of the Casimir energy as a function of geometrical size. In 1D, $E_C \sim \hbar v/L$ where v is the velocity. Now we will show that the Josephson current in a long SNS junction from a field-theoretical point of view can be considered as a manifestation of the Casimir effect. Namely, the Andreev boundary condition changes the energy of the «Fermi sea» of quasiparticles in the normal region. This results in the appearance of: (i) an additional cohesive force between the superconducting banks [30], and (ii) a supercurrent induced by the superconducting phase difference.

As a simple example we evaluate the Josephson current in a long transparent 1D SNS junction by using a field theoretical approach. Andreev scattering at the NS interfaces results in twisted periodic boundary conditions, Eq. (26), for the chiral fermion fields [51]. So the problem is reduced to the evaluation of the Casimir energy for chiral fermions on an S^1 manifold of circumference $2L$ with «flux» ϑ. Notice that the left- and right-moving quasiparticles feel opposite (in sign) «flux» (see Eq. (29)). The energy spectrum takes the form ($\Delta_L = \hbar v_F/L$)

$$E_{n,\eta}(L,\varphi) = \pi\Delta_L\left(n - \frac{1}{2} + \eta\frac{\varphi}{2\pi}\right),$$

$$n = 0, \pm1, \pm2, \ldots, \eta = \pm1, \quad (31)$$

and coincides (as it should be) with the electron and hole energies calculated by matching the quasiparticle wave functions at the NS boundaries [26]. The Casimir energy is defined as the shift of the vacuum energy induced by the boundary conditions

$$E_C(L,\varphi) = 2\left(-\frac{1}{2}\right)\left[\sum_{n,\eta}E_{n,\eta}(L,\varphi) - \sum_{n,\eta}E_{n,\eta}(L\to\infty)\right]. \quad (32)$$

Notice, that the factor $(-1/2)$ in Eq. (32) is due to the zero-point energy of chiral fermions, the additional factor of 2 is due to spin degeneracy. Both sums in Eq. (32) diverge and one needs a certain regularization procedure to manipulate them. One of the most efficient regularization methods in the calculation of vacuum energies is the so-called generalized zeta-function regularization [62]. For the simple energy spectrum, Eq. (31), this procedure is reduced to the analytical continuation of the infinite sum over n in Eq. (32) to the complex plane,

$$E_C(\varphi) = -\pi\Delta_L \lim_{s\to-1}\sum_{n=-\infty,\,\eta=\pm1}^{\infty}(n + a_\eta)^{-s} =$$

$$= -\pi\Delta_L\sum_{\eta=\pm1}[\zeta(-1,a_\eta) + \zeta(-1,-a_\eta) + a_\eta], \quad (33)$$

where $\zeta(s,a)$ is the generalized Riemann ζ-function [54] and $a_\eta = (\pi + \eta\varphi)/2\pi$. Using an expression for $\zeta(-n,a)$ in terms of Bernoulli polynomials that is well-known from textbooks (see Ref. 54) one gets the desired formula for the Casimir energy of a 1D SNS junction as

$$E_C = 2\pi \frac{\hbar v_F}{L}\left[\left(\frac{\varphi}{2\pi}\right)^2 - \frac{1}{12}\right], \ |\varphi| \le \pi . \qquad (34)$$

The Casimir force F_C and the Josephson current J at $T = 0$ are

$$F_C = -\frac{\partial E_C}{\partial \varphi} = \frac{E_C}{L}, \ J = \frac{e}{\hbar}\frac{\partial E_C}{\partial \varphi} = \frac{e v_F}{L}\frac{\varphi}{\pi}, \quad |\varphi| \le \pi. \qquad (35)$$

the expression for the Josephson current coincides with the zero-temperature limit of Eq. (30). The generalization of the calculation method to finite temperatures is straightforward. The additional cohesive force between two bulk metals induced by superconductivity is discussed in Ref. 30. In this paper it was shown that for a multichannel SNS junction this force can be measured in modified AFM-STM experiments, where force oscillations in nanowires were observed.

The calculation of the Casimir energy for a system of interacting electrons is a much more sophisticated problem. In Ref. 47 this energy and the corresponding Josephson current were analytically calculated for a special exactly solvable case of double-boundary LL. Unfortunately the considered case corresponds to the attractive regime of LLs ($g_\rho = 2$ in our notation, see Eq. (6)) and the interesting results obtained in Ref. 47 can not be applied for electron transport in quantum wires fabricated in 2DEG or in individual SWNTs were the electron–electron interaction is known to be repulsive.

3. The effects of Zeeman splitting and spin–orbit interaction in SNS junctions

In the previous Section we considered the influence of electron–electron interactions on the Josephson current in a S–QW–S junction. Although all calculations were performed for a spin-1/2 Luttinger liquid model, it is readily seen that the spin degrees of freedom in the absence of a magnetic field are trivially involved in the quantum dynamics of our system. In essence, they do not change the results obtained for spinless particles. For noninteracting electrons spin only leads to an additional statistical factor 2 (spin degeneracy) in the thermodynamic quantities. At the first glance spin effects could manifest themselves in SLLS junctions since it is known that in LL the phenomena of spin-charge separation takes a place [46]. One could naively expect some manifestations of this nontrivial spin dynamics in the Josephson current. Spin effects for interacting electrons are indeed not reduced to the appearance of statistical factor. However, as we have seen already in the previous sections, the dependence of the critical Josephson current on the interaction strength is qualitatively the same for spin-1/2 and spinless Luttinger liquids. So it is for ease of calculations a common practice to investigate weak superconductivity in the model of spinless Luttinger liquid [47].

Spin effects in the Josephson current become important in the presence of a magnetic field, spin–orbit interactions or spin–dependent scattering on impurities. At first we consider the effects induced by a magnetic field. Generally speaking a magnetic field influences both the normal part of the junction and the superconducting banks. It is the last impact that determines the critical Josephson current in short and wide junctions. The corresponding problem was solved many years ago and one can find the analytical results for a short and wide junction in a magnetic field parallel to the NS interface (e.g., in Refs. 63 and 64).

In this review we are interested in the superconducting properties of junctions formed by a long ballistic quantum wire coupled to bulk superconductors. We will assume that a magnetic field is applied locally, i.e., only to the normal part of the junction (such an experiment could be realized for instance with the help of a magnetic tip and a scanning tunneling microscope). In this case the only influence of the magnetic field on the electron dynamics in a single channel (or few channel) QW is due to the Zeeman interaction. For noninteracting electrons the Zeeman splitting lifts the double degeneracy of Andreev levels in an SNS junction and results in a periodic dependence of the critical Josephson current on magnetic field [65].

Interaction effects can easily be taken into account for a 1D SLLS junction in a magnetic field by using bosonization techniques. The term in the Hamiltonian $\hat{H}_Z$, which describes the interaction of the magnetic field $\mathbf{B}$ with the electron spin $\mathbf{S}(x)$ is in bosonized form (see, e.g., Ref. 46)

$$\hat{H}_Z = -g_f \mu_B B_z \int dx\, S_z(x), \ S_z(x) = \frac{1}{\sqrt{2\pi}}\partial_x \varphi_\sigma, \qquad (36)$$

where g_f is the g-factor, μ_B is the Bohr magneton and the scalar field φ_σ is defined in Eq. (16). As is easy to see, this interaction can be transformed away in the LL Hamiltonian by a coordinate-dependent shift of the spin bosonic field $\varphi_\sigma \Rightarrow \varphi_\sigma + \Delta_z x/\hbar v_F\sqrt{2\pi}$, $\Delta_z = g_f \mu_B B$ is the Zeeman splitting. So the Zeeman splitting introduces an extra x-dependent phase factor in the chiral components of the fermion fields and thus the Zeeman interaction can be readily taken into account [66] by a slight change of the bosonization formula (13)

$$\psi^{(Z)}_{\eta,\sigma}(x,t) = \exp(iK_{\eta,\sigma}x)\,\psi_{\eta,\sigma}(x,t),$$

$$K_{\eta,\sigma} = \frac{\Delta_z}{4\hbar v_F}\eta\sigma, \quad \eta,\sigma = \pm 1. \tag{37}$$

The phase factor appearing in Eq. (37) results in a periodic dependence of the Josephson current on magnetic field. In the presence of Zeeman splitting the critical current, say, for a tunnel SLLS junction, Eq. (21), acquires an additional harmonic factor $\cos(\Delta_Z/\Delta_L)$, the same as for noninteracting particles.

3.1. Giant critical current in a magnetically controlled tunnel junction

Interesting physics for low-transparency junctions appears when resonant electron tunneling occurs. In this subsection we consider the special situation when the conditions for resonant tunneling through a junction are induced by superconductivity. The device we have in mind is an SNINS ballistic junction formed in a 2DEG with a tunable tunnel barrier («*I*») and a tunable Zeeman splitting which can be provided for instance with the help of a magnetic tip and a scanning tunneling microscope (STM). In quantum wires fabricated in 2DEG the effects of electron–electron interactions are not pronounced and we will neglect them in what follows.

Resonant electron tunneling through a double barrier mesoscopic structure is a well studied quantum phenomenon, which has numerous applications in solid state physics. Recently a manifestation of resonant tunneling in the persistent current both in superconducting [67] and in normal systems [68] was studied. In these papers a double-barrier system was formed by the two tunnel barriers at the NS interfaces [67] or in a normal metal ring [68]. It was shown that for resonance conditions (realized for a special set of junction lengths [67] or interbarrier distances [68]) a giant persistent current appears which is of the same order of magnitude as the persistent current in a system with only a single barrier. In the case of the SINIS junction considered in Ref. 67 the critical supercurrent was found to be proportional to $\sqrt{D}$. Notice that the normal transmission coefficient for a symmetric double-barrier structure (i.e., the structure with normal leads) at resonance conditions does not depend on the barrier transparency at all. It means that for the hybrid structure considered in Ref. 67 the superconductivity actually suppresses electron transport.

Now we show [69] that in a magnetically controlled single barrier SFIFS junction («*F*» denotes the region with nonzero Zeeman splitting) there are conditions when superconductivity in the leads strongly enhances electron transport. Namely, the proposed hybrid SFIFS structure is characterized by a giant critical current $J_c \sim \sqrt{D}$. While the normal conductance G is proportional to D.

For a single barrier SFIFS junction of length L, where the barrier is located at a distance $l << L$ measured from the left bank, the spectrum of Andreev levels is determined from the transcendental equation [69]

$$\cos\frac{2E \pm \Delta_Z}{\Delta_L} + R\cos\frac{2E \pm \Delta_Z}{\Delta_{L-2l}} + D\cos\varphi = 0, \tag{38}$$

where $\Delta_x = \hbar v_F/x$ and $D + R = 1$, Δ_Z is the Zeeman splitting. In the limit $\Delta_Z = 0$ Eq. (38) is reduced to a well-known spectral equation for Andreev levels in a long ballistic SNS junction with a single barrier [40,70].

At first we consider the symmetric single-barrier junction, i.e., the case when the scattering barrier is situated in the middle of the normal region $l = L/2$. Then the second cosine term in the spectral equation is equal to one and Eq. (38) is reduced to a much simpler equation which is easily solved analytically. The evaluation of the Josephson current shows [69] that for $D << 1$ and for a discrete set of Zeeman splittings,

$$\Delta_Z^k = \pi(2k+1)\Delta_L, \quad k = 0, 1, 2, \ldots, \tag{39}$$

the resonance Josephson current (of order $\sqrt{D}$) is developed. At $T = 0$ it takes the form

$$J_r(\varphi) = \frac{ev_F}{L}\sqrt{D}\frac{\sin\varphi}{|\sin(\varphi/2)|}. \tag{40}$$

This expression has the typical form of a resonant Josephson current associated with the contribution of a single Andreev level [40]. One can interpret this result as follows. Let us assume for a moment that the potential barrier in a symmetric SNINS junction is infinite. Then the system breaks up into two identical INS-hybrid structures. In each of the two systems de Gennes–Saint-James energy levels with spacing $2\pi\Delta_L$ are formed [71]. For a finite barrier these levels are split due to tunneling with characteristic splitting energy $\delta \sim \sqrt{D}\Delta_L$. The split levels being localized already on the whole length L between the two superconductors are nothing but the Andreev–Kulik energy levels, i.e., they depend on the superconducting phase difference. Although the partial current of a single level is large ($\sim \sqrt{D}$) (see Refs. 40 and 67), the current carried by a pair of split levels is small ($\sim D$) due to a partial cancellation. At $T = 0$ all levels above the Fermi energy are empty and all levels below E_F are filled. So in a system without Zeeman splitting the partial cancellation of currents carried by pairs of tunnel–split energy levels results in a small critical current ($\sim D$). The Zeeman splitting Δ_Z of order Δ_L (see Eq. (39)) shifts two sets («spin-up» and «spin-down») of Andreev levels so that the Fermi en-

ergy lies in between the split levels. Now at $T = 0$ only the lower state is occupied and this results in an uncompensated large ($\sim \sqrt{D}$) Josephson current. Since the quantized electron-hole spectrum is formed by Andreev scattering at the NS interfaces, the resonance structure for a single barrier junction disappears when the leads are in the normal (non-superconducting) state. So, the electron transport through the normal region is enhanced by superconductivity. Electron spin effects (Zeeman splitting) are crucial for the generation of a giant Josephson current in a single barrier junction.

The described resonant transport can occur not only in symmetric junction. For a given value of Zeeman splitting $\Delta_Z^{(k)}$ from Eq. (39) there is a set of points [69] (determined by their coordinates $x_m^{(k)}$ counted from the middle of the junction)

$$x_m^{(k)} = \pm \frac{m}{2k+1} L \qquad (41)$$

(m is the integer in the interval $0 \le m \le k + 1/2$), where a barrier still supports resonant transport. The temperature dependence of the giant Josephson current is determined by the energy scale $\delta \sim \sqrt{D}\Delta_L$ and therefore at temperatures $T \sim \delta$, which are much lower then Δ_L, all resonance effects are washed out.

3.2. Giant magnetic response of a quantum wire coupled to superconductors

It is known that the proximity effect produced in a wire by superconducting electrodes strongly enhances the normal conductance of the wire for certain value of the superconducting phase difference (giant conductance oscillations [72]). For ballistic electron transport this effect has a simple physical explanation [73] in terms of Andreev levels. Consider a multichannel ballistic wire perfectly (without normal electron backscattering) coupled to bulk superconductors. The wire is assumed to be connected to normal leads via tunnel contacts. In the first approximation one can neglect the electron leakage through the contacts and then the normal part of the considered Andreev interferometer is described by a set of Andreev levels produced by superconducting mirrors . When the distance L between the mirrors is much longer then the superconducting coherence length $L >> \xi_0 = \hbar v_F/\Delta$ (Δ is the superconducting gap), the spectrum takes a simple form [26]

$$E_{n,\pm}^{(j)} = \frac{\hbar v_F^{(j)}}{2L}[\pi(2n+1) \pm \varphi], \; n = 0, \pm 1, \pm 2, \ldots, \qquad (42)$$

where $v_F^{(j)}$ is the Fermi velocity of the jth transverse channel ($j = 1, 2, \ldots, N_\perp$). It is evident from Eq. (42) that at special values of phase difference $\varphi_n = \pi(2n+1)$ energy levels belonging to different transverse channels j, collapse to a single multi-degenerate ($N_\perp$) level exactly at the Fermi energy. So resonant normal electron transport through a multichannel wire (the situation which is possible for symmetric barriers in the normal contacts) will be strongly enhanced at $\varphi = \varphi_n$. The finite transparency of the barriers results in a broadening and a shift of the Andreev levels. These effects lead to a broadening of the resonance peaks in giant conductance oscillations at low temperatures [73].

Magnetic properties of a quantum wire coupled to superconductors can also demonstrate a behavior analogous to the giant conductance oscillations. We consider a long perfectly transmitting SNS junction in a local (applied only to the normal region) magnetic field. In this case the only influence of the magnetic field on the Andreev level structure is through the Zeeman coupling. The thermodynamic potential $\Omega_A(\varphi, B)$ calculated for Zeeman-split Andreev levels is [30]

$$\Omega_A(\varphi, B) = 4T \sum_{\{j\}}^{N_\perp} \sum_{k=1}^{\infty} \frac{(-1)^k}{k} \frac{\cos k\varphi \cos k\chi_j}{\sinh(2\pi kT/\Delta_L^{(j)})}. \qquad (43)$$

Here $\chi_j = \Delta_Z/\Delta_L^{(j)}$, $\Delta_Z = g\mu_B B$ is the Zeeman energy splitting, $\Delta_L^{(j)} = \hbar v_F^{(j)}/L$ and $v_F^{(j)}$ is the Fermi velocity in the jth transverse channel, $\{j\}$ is the set of transverse quantum numbers. In Ref. 30 the normal part of the SNS junction was modelled by a cylinder of length L and cross-section area $S = V/L$. Hard-wall boundary conditions for the electron wave function on the cylinder surface were assumed. Then the set $\{j\}$ is determined by the quantum numbers (l, n) that label the zeroes $\gamma_{l,n}$ of the Bessel function $J_l(\gamma_{l,n}) = 0$ and the velocity $v_F^{(l,n)}$ takes the form

$$v_F^{(l,n)} = \sqrt{\frac{2}{m}\left(\varepsilon_F - \gamma_{ln}^2 \frac{\pi\hbar^2 L}{2mV}\right)}. \qquad (44)$$

It is evident from Eq. (43) that the superconductivity-induced magnetization

$$M_A = -\frac{\partial \Omega_A(\varphi, B)}{\partial B} \qquad (45)$$

at high temperatures ($T >> \Delta_L$) is exponentially small and does not contribute to the total magnetization of the junction. At low temperatures T the magnetization peaks at $M_A \sim N_\perp g\mu_B$ where the superconducting phase difference is an odd multiples of π (see Fig. 6 which is adapted from Ref. 30). The qualitative explanation of this resonance behavior of the magnetization is as follows. It is known [74] that for $\varphi = \varphi_n \equiv (2n+1)\pi$ (n is the integer) the two Andreev levels $E_A^{(\pm)} = \pm\Delta_Z/2$ become $2N_\perp$-fold degenerate.

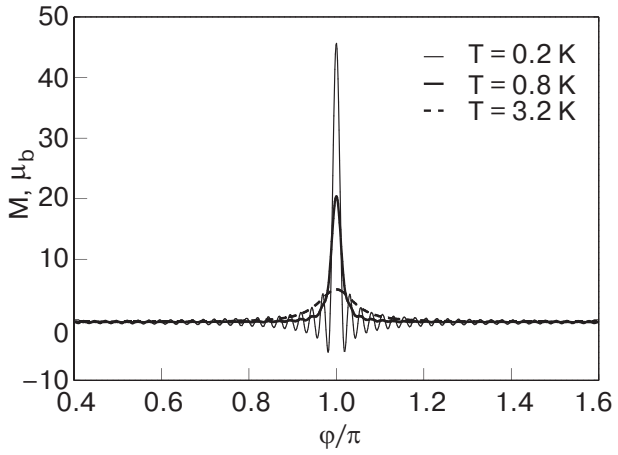

Fig. 6. Dependence of the magnetization M of an SNS junction on the superconducting phase difference for different temperatures.

At $T \to 0$ the filled state $E_A^{(-)}$ dominates in the magnetization at $\varphi = \varphi_n$ since at other values of superconducting phase the sets of Andreev levels corresponding to different transverse channels contribute to magnetization Eqs. (43), (45) with different periods in «magnetic phase» χ_j (i.e., in general, incoherently) and their contributions partially cancel each other. Notice also that for a fixed volume V, the number of transverse channels $N_\perp$ has a step-like dependence on the wire diameter. So at resonance values of the phase difference $\varphi = \varphi_n$ one can expect a step-like behavior of the magnetization as a function of wire diameter [30]. This effect is a magnetic analog of the Josephson current quantization in a short SNS junction [39] considered in Sec. 2.1.

3.3. Rashba effect and chiral electrons in quantum wires

Another type of system where spin is nontrivially involved in the quantum dynamics of electrons are conducting structures with strong spin–orbit interaction. It has been known for a long time [29] that the SO interaction in the 2DEG formed in a GaAs/AlGaAs inversion layer is strong due to the structural inversion asymmetry of the heterostructure. The appearance in quantum heterostructures of an SO coupling linear in electron momentum is now called the Rashba effect. The Rashba interaction is described by the Hamiltonian

$$H_{so}^{(R)} = i\alpha_{SO}\left(\sigma_y \frac{\partial}{\partial x} - \sigma_x \frac{\partial}{\partial y}\right), \qquad (46)$$

where $\sigma_{x(y)}$ are the Pauli matrices. The strength of the spin–orbit interaction is determined by the coupling constant α_{so}, which ranges in a wide interval $(1-10)\cdot 10^{-10}$ eV·cm for different systems (see, e.g., Ref. 31 and references therein). Recently it was experimentally shown [75–77] that the strength of the Rashba interaction can be controlled by a gate voltage $\alpha_{so}(V_G)$. This observation makes the Rashba effect a very attractive and useful tool in spintronics. The best known proposal based on the Rashba effect is the spin-modulator device of Datta and Das [78].

The spin–orbit interaction lifts the spin degeneracy of the 2DEG energy bands at $\mathbf{p} \neq 0$ ($\mathbf{p}$ is the electron momentum). The Rashba interaction, Eq. (46) produces two separate branches for «spin-up» and «spin-down» electron states

$$\varepsilon(\mathbf{p}) = \frac{\mathbf{p}^2}{2m} \pm \frac{\alpha_{SO}}{\hbar}|\mathbf{p}|. \qquad (47)$$

Notice that under the conditions of the Rashba effect the electron spin lies in a 2D plane and is always perpendicular to the electron momentum. By the terms «spin-up» («spin-down») we imply two opposite spin projections at a given momentum. The spectrum (47) does not violate left-right symmetry, that is the electrons with opposite momenta ($\pm\mathbf{p}$) have the same energy. Actually, the time reversal symmetry of the spin–orbit interaction, Eq. (46), imposes less strict limitations on the electron energy spectrum, namely, $\varepsilon_\sigma(-\mathbf{p}) = \varepsilon_{-\sigma}(\mathbf{p})$ and thus, the Rashba interaction can in principle break the chiral symmetry. In [31] it was shown that in quasi-1D quantum wires formed in a 2DEG by a laterally confining potential the electron spectrum is characterized by a dispersion asymmetry $\varepsilon_\sigma(-\mathbf{p}) \neq \varepsilon_\sigma(\mathbf{p})$. It means that the electron spectrum linearized near the Fermi energy is characterized by two different Fermi velocities $v_{1(2)F}$ and, what is more important, electrons with large (Fermi) momenta behave as chiral particles in the sense that in each subband (characterized by Fermi velocity $v_F^{(1)}$ or $v_F^{(2)}$) the direction of the electron motion is correlated with the spin projection [31,79] (see Fig. 7). It is natural in this case to characterize the spectrum by the asymmetry parameter

$$\lambda_a = \frac{v_{1F} - v_{2F}}{v_{1F} + v_{2F}}, \qquad (48)$$

which depends on the strength of Rashba interaction $\lambda_a(\alpha_{SO} = 0) = 0$. The asymmetry parameter grows with the increase of α_{SO} and can be considered in this model as the effective dimensional strength of the Rashba interaction in a 1D quantum wire [31]. Notice that the spectrum proposed in [31,79] (Fig. 7, solid lines for spin projections) does not hold for strong SO interactions, when λ_a is not small. Spin is not conserved in the presence of the SO interaction and the prevailing spin projection of electron states in quasi 1D wires has to be independently calculated. It was shown in Ref. 32 by a direct calculation of the average

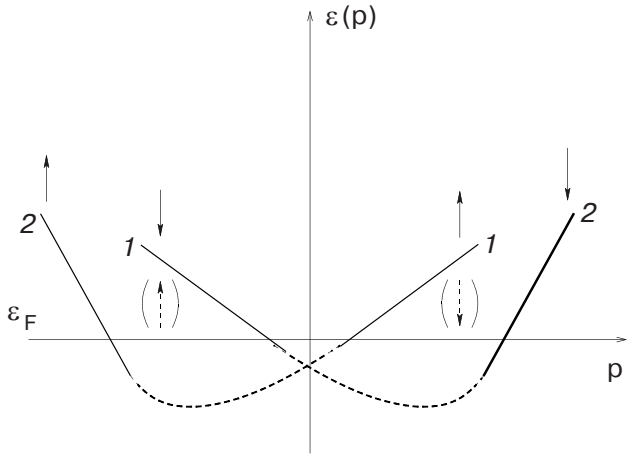

Fig. 7. Schematic energy spectrum of 1D electrons with dispersion asymmetry. Particles with energies close to the Fermi energy ε_F have an almost linear dependence on momentum and are classified by their Fermi velocities (v_{1F}-subband *1*, v_{2F}-subband *2*). Solid line for spin projections correspond to the case of weak SO interaction; spin in parentheses indicates the spin projections in subband *1* for strong Rashba interaction.

electron spin projection that for energies close to ε_F the electron spin projection for strong Rashba interaction (comparable with the band splitting in the confining potential) is strongly correlated with the direction of the electron motion. Namely, the right (R)-and the left (L)-moving electrons always have opposite spin projections regardless of their velocities (see Fig. 7, where the parentheses indicate the spin projection for strong Rashba interaction). For our choice of Rashba SO Hamiltonian, Eq. (46), R-electrons ($k_x > 0$) will be «down-polarized» ($< \sigma_y > = -1$) and L-electrons ($k_x < 0$) will be «up-polarized» ($< \sigma_y > = +1$) to minimize the main part of electron energy $\sim (\hbar^2/2m) < k_x + \sigma_y m\alpha_{SO}/\hbar >^2$ in the presence of strong spin–orbit interaction [32].

Chiral electrons in 1D quantum wire result in such interesting predictions as «spin accumulation» in normal wires [32] or Zeeman splitting induced supercurrent in S–QW–S junction [69].

3.4. Zeeman splitting induced supercurrent

It was shown in the previous subsection that under the conditions of the Rashba effect in 1D quantum wires the spin degree of freedom is strongly correlated with the electron momentum. This observation opens the possibility to magnetically control an electric current. It is well known that in ring-shaped conductors the current can be induced by magnetic flux due to the momentum dependent interaction of the electromagnetic potential **A** with a charged particle $H_{\rm int} = (e/mc)\mathbf{pA}$. Chiral properties of electrons in quasi-1D quantum wires allow one to induce a persistent current via pure spin (momentum independent) interaction $H = g\mu_B \mathbf{SH}$. Below we consider the Josephson current in a ballistic S–QW–S junction in the presence of Rashba spin–orbit interaction and Zeeman splitting. We will assume at first that SO interactions exist both in the normal part of the junction and in the superconducting leads, so that one can neglect the spin rotation accompanied by electron backscattering induced by SO interactions at the NS interfaces. In other words the contacts are assumed to be fully adiabatic. This model can be justified at least for a weak SO interaction. The energy spectrum of electrons in a quantum wire is shown in Fig. 7 and the effect of the SO interaction in this approach is characterized by the dispersion asymmetry parameter λ_a, Eq. (48).

For a perfectly transparent junction ($D = 1$) the two subbands *1* and *2* (see Fig. 7) contribute independently to the Andreev spectrum which is described by two sets of levels [69]

$$E^{(1)}_{n,\eta} = \pi\Delta^{(1)}_L \left(n + \frac{1}{2} + \eta \frac{\varphi + \chi_1}{2\pi} \right),$$
$$E^{(2)}_{m,\eta} = \pi\Delta^{(2)}_L \left(m + \frac{1}{2} + \eta \frac{\varphi - \chi_2}{2\pi} \right), \qquad (49)$$

where the integers $n, m = 0, \pm 1, \pm 2, \ldots$ are ordinary quantum numbers which label the equidistant Andreev levels in a long SNS junction [26], $\eta = \pm 1$, $\Delta^{(j)}_L = \hbar v_{jF}/L$ ($j = 1, 2$) and φ is the superconducting phase difference. The magnetic phases $\chi_j = \Delta_Z/\Delta^{(j)}_L$ characterize the shift of Andreev energy levels induced by Zeeman interaction. Notice that the relative sign between the superconducting phase φ and the magnetic phase χ_j is different for channels *1* and *2*. This is a direct consequence of the chiral properties of the electrons in our model. In the absence of a dispersion asymmetry ($v_{1F} = v_{2F} \equiv v_F$) the two sets of levels in Eq. (49) describe the ordinary spectrum of Andreev levels in a long transparent SFS junction («F» stands for the normal region with Zeeman splitting)

$$E_{n,\eta,\sigma} = \pi\Delta_L \left(n + \frac{1}{2} + \eta \frac{\varphi}{2\pi} + \sigma \frac{\chi}{2\pi} \right), \quad \eta, \sigma = \pm 1. \qquad (50)$$

Knowing explicitly the energy spectrum, Eq. (49), it is straightforward to evaluate the Josephson current. It takes the form [69]

$$J(\varphi, T, \Delta_Z) = \frac{2eT}{\hbar} \sum_{k=1}^{\infty} (-1)^{k+1} \left[\frac{\sin k(\varphi + \chi_1)}{\sinh(2\pi kT/\Delta^{(1)}_L)} + \frac{\sin k(\varphi - \chi_2)}{\sinh(2\pi kT/\Delta^{(2)}_L)} \right]. \qquad (51)$$

Here T is the temperature. The formal structure of Eq. (51) is obvious. The two sums in Eq. (51) correspond to the contributions of magnetically shifted sets of levels 1 and 2 in Eq. (49). In the absence of any SO interaction the Zeeman splitting results only in an additional $\cos(k\Delta_Z/\Delta_L)$ factor in the standard formula for the supercurrent through a perfectly transmitting long SNS junction [57]. The most striking consequence of Eq. (51) is the appearance of an anomalous Josephson current $J_{an} \equiv J(\varphi = 0)$, when both the Zeeman splitting (Δ_Z) and dispersion asymmetry (λ_a) are nonzero. At high temperatures $T \geq \Delta_L^{(j)}$ the anomalous supercurrent is exponentially small. In the low temperature regime $T << \Delta_L^{(j)}$ it is a piece-wise constant function of the Zeeman energy splitting Δ_Z,

$$J_{an}(\Delta_Z) = \frac{e}{\pi L}\sum_{k=1}^{\infty}\frac{(-1)^{k+1}}{k}\left[v_{1F}\sin\left(k\frac{\Delta_Z}{\Delta_L^{(1)}}\right) - v_{2F}\sin\left(k\frac{\Delta_Z}{\Delta_L^{(2)}}\right)\right]. \quad (52)$$

For rational values $v_{1F}/v_{2F} = p/q$ ($p \leq q$ are the integers) J_{an} is a periodic function of the Zeeman energy splitting with period $\delta\Delta_Z = 2\pi q\Delta_L^{(1)}$, otherwise it is a quasiperiodic function. The dependence of the normalized supercurrent J_{an}/J_0 (here $J_0 = ev_F/L$, $v_F = (v_{1F} + v_{2F})/2$) on the dimensionless Zeeman splitting $\chi \equiv \Delta_Z/\Delta_L$ for $\lambda_a = 0.1$ and for different temperatures is shown in Fig. 8. We see that at $T = 0$ the Zeeman splitting induced supercurrent appears abruptly at finite values of Δ_Z of the order of the Andreev level spacing.

Let us imagine now the situation when the Zeeman splitting arises due to a local magnetic field (acting only on the normal part of the junction) in the 2D plane applied normal to the quantum wire. Then the vector product of this magnetic field and the electric field (normal to the plane), which induces the Rashba interaction determines the direction of the anomalous supercurrent. In other words the change of the sign of the SO interaction in Eq. (46) or the sign of Δ_Z makes the supercurrent Eq. (52) change sign as well.

Now we briefly discuss the case of a strong Rashba interaction (the characteristic momentum $k_{SO} = m/\hbar\alpha_{SO}(V_g)$ is of the order of the Fermi momentum). The electrons in a quantum wire with strong Rashba coupling are chiral particles, that is the right- and left-moving particles have opposite spin projections [32]. There is no reason to assume a strong SO interaction in 3D superconducting leads. We will follow the approach taken in [32,80], where the system was modelled by a quantum wire ($\alpha_{SO} \neq 0$) attached to semi-infinite leads with $\alpha_{SO} = 0$. In this model the SN interface acts as a special strong scatterer where backscattering is accompanied by spin-flip process. For a general nonresonant situation the dispersion asymmetry is not important in the limit of strong Rashba interaction and we can put $v_{1F} \approx v_{2F} \approx v_F$. Then the Josephson current at $T = 0$ up to numerical factor takes the form

$$J(\varphi, \Delta_Z) \approx D_{\text{eff}}(\alpha_{SO})\frac{ev_F}{L}\sin\left(\varphi + \frac{\Delta_Z}{\Delta_L}\right). \quad (53)$$

Here $D_{\text{eff}}(\alpha_{SO}) << 1$ is the effective transparency of the junction. It can be calculated by solving the transition problem for the corresponding normal junction [32]. Anyway, in the considered model for NS interfaces (nonadiabatic switching on the Rashba interaction) even in the limit of strong Rashba interaction the anomalous supercurrent $J_{an} = J(\varphi = 0, \Delta_Z)$ is small because of smallness of the effective transparency of the junction. One could expect large current only for special case of resonant transition. This problem has not yet been solved.

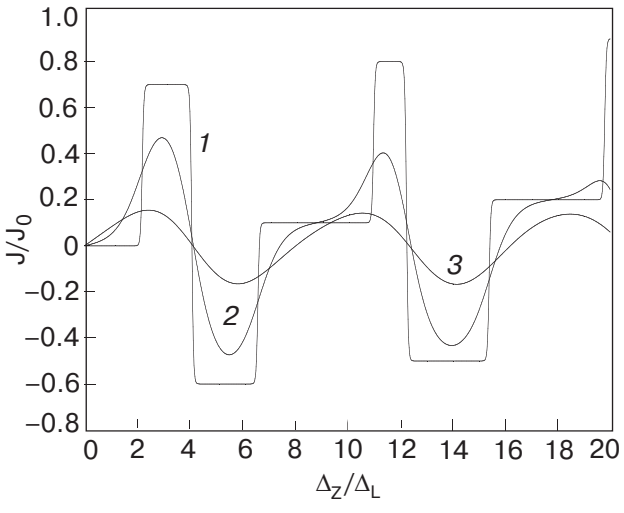

Fig. 8. Dependence of the normalized anomalous Josephson current J_{an}/J_0 ($J_0 = ev_F/L$) on the dimensionless Zeeman splitting Δ_z/Δ_L ($\Delta_L = \hbar v_F/L$) for asymmetry parameter $\lambda_a = 0.1$. The different plots correspond to different temperatures T: $0.1T^*(1)$; $1.5T^*(2)$; $3.5\ T^*(3)$, where $T^* = \Delta_L/2\pi$.

4. Conclusion

The objective of our review was to discuss the qualitatively new features of the Josephson effect that appear in S–QW–S hybrid structures. Quantum wires are characterized by a 1D or quasi-1D character of the electron conductivity. Electron transport along QWs is ballistic and due to the weak screening of the Coulomb interaction in 1D it is described by a Luttinger liquid theory. So the first question we would like to answer was — what is the Josephson effect in SLLS junction? It was shown that although electrons do not propagate in a LL weak link the supercurrent in a perfectly transmitting SLLS junction exactly coincides with the one in an SNS junction [22]. This «no renormalization» theorem is analogous to the result known for a LL adiabatically coupled to nonsuperconducting leads [35]. For a tunnel SILLIS junction the dc Josephson current is described by the famous Josephson current-phase relation, however now the effective transparency $D_{\text{eff}} << 1$ defined as $J = J_0 D_{\text{eff}} \sin\varphi$ (where $J_0 = ev_F/L$) strongly depends on the aspect ratio of the LL wire d/L ($d \sim \lambda_F$ is the width of the nanowire), temperature and electron–electron interaction strength. This result [21] is a manifestation of the Kane–Fisher effect [34] in mesoscopic superconductivity. It was also interesting for us (and we hope for the readers as well) to find a close connection, rooted in the Andreev boundary conditions, between the physics of a long SNS junction and the Casimir effect (see Sec. 2.3.).

Qualitatively new behavior of the proximity induced supercurrent in nanowires is predicted for systems with strong spin–orbit interactions. The Rashba effect in nanowires results in the appearance of chiral electrons [31,32] for which the direction of particle motion along the wire (right or left) is strongly correlated with the electron spin projection. For chiral electrons the supercurrent can be magnetically induced via Zeeman splitting. The interplay of Zeeman, Rashba interactions and proximity effects in quantum wires leads to effects that are qualitatively different from those predicted for 2D junctions [81].

It is worth-while to mention here another important trend in mesoscopic superconductivity, namely, the fabrication and investigation of superconductivity-based qubits. Among different suggestions and projects in this rapidly developing field, the creation of a so-called single–Cooper–box (SCPB) was a remarkable event [82]. The SCPB consist of an ultrasmall superconducting dot in tunneling contact with a bulk superconductor. A gate electrode, by lifting the Coulomb blockade of Cooper-pair tunneling, allows the delocalization of a single Cooper pair between the two superconductors. For a nanoscale grain the quantum fluctuations of the charge on the island are suppressed due to the strong charging energy associated with a small grain capacitance. By appropriately biasing the gate electrode it is possible to make the two states on the dot, differing by one Cooper pair, have the same energy. This twofold degeneracy of the ground state brings about the opportunity to create a long-lived coherent mixture of two ground states (qubit).

The superconducting weak link which includes a SCPB as a tunnel element could be very sensitive to external ac fields. This problem was studied in [83], where the resonant microwave properties of a voltage biased single–Cooper–pair transistor were considered. It was shown that the quantum dynamics of the system is strongly affected by interference between multiple microwave-induced inter-level transitions. As a result the magnitude and the direction of the dc Josephson current are extremely sensitive to small variations of the bias voltage and to changes in the frequency of the microwave field. This picture, which differs qualitatively from the famous Shapiro effect [3], is a direct manifestation of the role the strong Coulomb correlations play in the nonequilibrium superconducting dynamics of mesoscopic weak links.

Acknowledgment

The authors thank E. Bezuglyi, L. Gorelik, A. Kadigrobov, and V. Shumeiko for numerous fruitful discussions. Ilya V. Krive and Sergei I. Kulinich acknowledge the hospitality of the Department of Applied Physics at Chalmers University of Technology and Göteborg University. Financial support from the Royal Swedish Academy of sciences (Sergei I. Kulinich), the Swedish Science Research Council (Robert I. Shekhter) and the Swedish Foundation for Strategic Research (Robert I. Shekhter and Mats Jonson) is gratefully acknowledged.

1. B.D. Josephson, *Phys. Lett.* **1**, 251 (1962).
2. P.W. Anderson and J.M. Rowell, *Phys. Rev. Lett.* **10**, 230 (1963).
3. S. Shapiro, *Phys. Rev. Lett.* **11**, 80 (1963).
4. I.K. Yanson, V.M. Svistunov, and I.M. Dmitrenko, *Sov. Phys. JETP* **48**, 976 (1965); I.K. Yanson, V.M. Svistunov, and I.M. Dmitrenko, *Zh. Eksp. Teor. Fiz.* **47**, 2091 (1964) [*Sov. Phys. JETP* **20**, 1404 (1965)].
5. I.O. Kulik and I.K. Yanson, *Josephson Effect in Superconducting Tunnel Structures*, Nauka, Moscow (1970) (in Russian).
6. R. Saito, G. Dresselhaus, and M.S. Dresselhaus, *Physical Properties of Carbon Nanotubes*, Imperial College Press, London (1998).
7. S.J. Tans et al., *Nature* **386**, 474 (1997).
8. M. Bockrath et al., *Science* **275**, 1922 (1997).
9. A. Bachtold et al., *Phys. Rev. Lett.* **84**, 6082 (2000).

10. C. Dekker, *Phys. Today* (1999), p.22.
11. R.E. Peierls, *Quantum Theory of Solids*, Oxford University Press, New York (1955).
12. R. Egger and A.O. Gogolin, *Phys. Rev. Lett.* **79**, 5082 (1997), *Eur. Phys. J.* **B3**, 281 (1998).
13. C.L. Kane, L. Balents, and M.P.A. Fisher, *Phys. Rev. Lett.* **79**, 5086 (1997).
14. M. Bockrath et al., *Nature* **397**, 598 (1999).
15. H.W.C. Postma et al., *Phys. Rev.* **B62**, R10653 (2000).
16. H. Ishii et al., *Nature* **402**, 540 (2003).
17. M. Kociak et al., *Phys. Rev. Lett.* **86**, 2416 (2001).
18. A.Yu. Kasumov et al., *Physica* **B329–333**, 1321 (2003).
19. A.Yu. Kasumov et al., *Science* **284**, 1508 (1999).
20. A.F. Morpurgo et al., *Science* **286**, 263 (1999).
21. R. Fazio, F.W.J. Hekking, and A.A. Odintsov, *Phys. Rev. Lett.* **74** 1843 (1995).
22. D.L. Maslov et al., *Phys. Rev.* **B53**, 1548 (1996).
23. I. Affleck, J.S. Caux, and A.M. Zagoskin, *Phys. Rev.* **B62**, 1433 (2000).
24. H. van Houten and C. Beenakker, *Phys. Today* **49**, 22 (1996).
25. S. Tarucha et al., *Solid State Commun.* **94**, 413 (1995); A. Yacoby et al., *Phys. Rev. Lett.* **77**, 4612 (1996).
26. I.O. Kulik, *Zh. Eksp. Teor. Fiz.* **57**, 1745 (1969) [*Sov. Phys. JETP* **30**, 944 (1970)].
27. I.O. Kulik, *Sov. Phys. JETP* **22**, 841 (1966).
28. B.I. Spivak and S.A. Kivelson, *Phys.Rev.* **B43**, (1991).
29. E.I. Rashba, *Fiz. Tverd. Tela* (*Leningrad*) **2**, 1224 (1960) [*Sov. Phys. Solid State* **2**, 1109 (1960)]; Yu.A. Bychkov and E.I. Rashba, *J. Phys.* **C17**, 6039 (1984).
30. I.V. Krive, I.A. Romanovsky, E.N. Bogachek, and Uzi Landman, *Phys. Rev. Lett.* **92**, 126802 (2004).
31. A.V. Moroz and C.H.W. Barnes, *Phys. Rev.* **B60**, 14272 (1999).
32. M. Governale and U. Zulicke, *Phys. Rev.* **B66**, 073311 (2002).
33. S. Datta, *Electronic Transport in Mesoscopic Systems*, Cambridge University Press, Cambridge (1995).
34. C.L. Kane and M.P.A. Fisher, *Phys. Rev. Lett.* **68**, 1220 (1992).
35. D.L. Maslov and M. Stone, *Phys. Rev.* **B52**, R5539 (1995); V.V. Ponomarenko, *Phys. Rev.* **B52**, R8666 (1995); I. Safi and H.J. Schulz, *Phys. Rev.* **B52**, R17040 (1995).
36. C.L. Kane and M.P.A. Fisher, *Phys. Rev.* **B46**, 15233 (1992); A. Furusaki and N. Nagaosa, *Phys. Rev.* **B47**, 3827 (1993).
37. M.P.A. Fisher and L.I. Glazman, in: *Mesoscopic Electron Transport, Vol. 345 of NATO Advanced Study Institute, Series E: Applied Sciences,* L.L. Sohn, L.P. Kouwenhoven, and G. Schon (eds.), Kluwer Academic Publishing, Dordrecht (1997).
38. A. Furusaki and M. Tsukuda, *Physica* **B165–166**, 967 (1990); S.K. Kuplevakhskii and I.I. Fal'ko, *Fiz. Nizk. Temp.* **17**, 961 (1991) [*Sov. J. Low. Temp. Phys.* **17**, 501 (1991)].
39. C.W.J. Beenaker and H. van Houten, *Phys. Rev. Lett.* **66**, 3056 (1991).
40. P. Samuelsson et al., *Phys. Rev.* **B62**, 1319 (2000).
41. B.J. van Wees et al., *Phys. Rev. Lett.* **60**, 848 (1988); D.A. Wharam et al., *J. Phys.* **C21**, L209 (1988).
42. L. Glazman et al., *Pisma Zh. Eksp. Teor. Fiz*, **48**, 329 (1988) [*JETP Letters,* **48**, 238 (1988)].
43. K.A. Matveev et al., *Phys. Rev. Lett.* **70**, 2940 (1993).
44. K. Engstom et al., *Low Temp. Phys.* **29**, 546 (2003).
45. A.F. Andreev, *Zh. Eksp. Teor. Fiz.* **46**, 1863 (1964) [*Sov. Phys. JETP* **19**, 1228 (1964)]; *ibid* **49**, 655 (1965).
46. A.O. Gogolin, A.A. Nersesyan, and A.M. Tsvelik, *Bosonization and Strongly Correlated Systems*, Cambridge University Press (1988).
47. J.S. Caux, H. Saleur, and F. Siano, *Phys. Rev. Lett.* **88**, 106402 (2002).
48. A.L. Shelankov, *Pis'ma Zh. Eksp. Teor. Fiz.* **32**, 122 (1980) [*JETP Letters* **32**, 111 (1980)].
49. G.E. Blonder, M. Tinkham, and T.M. Klapwijk, *Phys. Rev.* **B25**, 4515 (1982).
50. M. Fabrizio and A.O. Gogolin, *Phys. Rev.* **B51**, 17827 (1995).
51. D. Loss, *Phys. Rev. Lett.* **69**, 343 (1992).
52. J.S. Caux, A. Lopez, and D. Suppa, *Nucl. Phys.* **B651**, 413 (2003).
53. R. Egger et al., in: *Interacting Electrons in Nanostructures*, R. Haug and H. Schoeller (eds.), Springer (2000); *cond-mat/0008008* (2000).
54. I.S. Gradshteyn and I.M. Ryzhik, *Tables of Integrals Series and Products*, Academic Press, New York and London (1965).
55. I.V. Krive et al., *Phys. Rev.* **B52**, 16451 (1995).
56. A.A. Zvyagin and I.V. Krive, *Fiz. Nizk. Temp.* **21**, 687 (1995).
57. C. Ishii, *Prog. Theor. Phys.* **44**, 1525 (1970); A.V. Svidzinsky, T.N. Antsygina, and E.N. Bratus, *Zh. Eksp. Teor. Fiz.* **61**, 1612 (1971) [*Sov. Phys. JETP* **34**, 860 (1972)].
58. H.B.G. Casimir, *Kon. Ned. Akad. Wetensch. Proc.* **51**, 793 (1948).
59. V.M. Mostepanenko and N.N. Trunov, *The Casimir Effect and its Application*, Claredon Press, Oxford (1977).
60. K.A. Milton, *The Casimir Effect: Physical Manifestation of Zero-Point Energy*, World Scientific (2001).
61. G. Bressi et al., *Phys. Rev. Lett.* **88**, 041804 (2002).
62. S.W. Hawking, *Commun. Math. Phys.* **55**, 133 (1977).
63. V.P. Galaiko and E. V. Bezuglyi, *Zh. Eksp. Teor. Fiz.* **60**, 1471 (1971); G.A. Gogadze and I.O. Kulik, *Zh. Eksp. Teor. Fiz.* **60**, 1819 (1971).
64. A.V. Svidzinsky, *Inhomogeneous Problems in a Theory of Superconductivity,* Nauka, Moscow (1982) [in Russian].
65. A.I. Buzdin, L. N. Bulayevski, and S.V. Panyukov, *Pis 'ma Zh. Eksp. Teor. Fiz.* **35**, 147 (1982).
66. A.De Martino and R. Egger, *Europhys. Lett* **56**, 570 (2001).
67. G. Wendin and V.S. Shumeiko, *Phys. Rev.* **B53**, R6006 (1996); *Superlattices Microstruct.* **4**, 569 (1996).
68. P. Sandstrom and I.V. Krive, *Phys. Rev.* **B56**, 9255 (1997).

69. I.V. Krive, L.Y. Gorelik, R.I. Shekhter, and M. Jonson, *Fiz. Nizk. Temp.* **30**, 535 (2004).
70. P.F. Bagwell, *Phys. Rev.* **B46**, 12573 (1992).
71. P.G. de Gennes and D. Saint-James, *Phys. Lett.* **4**, 151 (1963).
72. V.T. Petrashov et al., *Phys. Rev. Lett.* **70**, 347 (1993).
73. A. Kadigrobov et al., *Phys. Rev.* **B52**, R8662 (1995); H.A. Blom et al., *Phys. Rev.* **B57**, 9995 (1998).
74. A. Kadigrobov et al., *Phys. Rev.* **B60**, 14593 (1999).
75. J. Nitta et al., *Phys. Rev. Lett.* **78**, 1335 (1997).
76. T. Schapers et al., *J. Appl. Phys.* **83**, 4324 (1998).
77. D. Grundler, *Phys. Rev. Lett.* **84**, 6074 (2000).
78. S. Datta and B. Das, *Appl. Phys. Lett.* **56**, 665 (1990).
79. A.V. Moroz, K.V. Samokhin, and C.H.W. Barnes, *Phys. Rev. Lett.* **84**, 4164 (2000); *Phys. Rev.* **B62**, 16900 (2000).
80. F. Mireles and G. Kirczenow, *Phys. Rev.* **B64**, 024426 (2001).
81. E.V. Bezuglyi et al., *Phys. Rev.* **B66**, 052508 (2002).
82. Y. Nakamura et al., *Nature* **398**, 786 (1999); A. Cottet et al., *Physica* **C367**, 197 (2002).
83. L.Y. Gorelik et al., *Phys. Rev.* **B69**, 094516 (2004).